Nucleosides and Nucleotides. 141. Chemical Stability of a New Antitumor Nucleoside, 2′-*C*-Cyano-2′-deoxy-1-β-D-*arabino*-pentofuranosylcytosine in Alkaline Medium: Formation of 2′-*C*-Cyano-2′-deoxy-1-β-D-*ribo*-pentofuranosylcytosine and Its Antitumor Activity[1]

Atsushi Azuma,[†] Kenji Hanaoka,[‡] Atsushi Kurihara,[§] Tomowo Kobayashi,[‡] Seiji Miyauchi,[†] Naoki Kamo,[†] Motohiro Tanaka,[∥] Takuma Sasaki,[∥] and Akira Matsuda*,[†]

Faculty of Pharmaceutical Sciences, Hokkaido University, Kita-12, Nishi-6, Kita-ku, Sapporo 060, Japan, Biological Research Laboratories and Product Development Laboratories, Sankyo Company, Ltd., Hiromachi, Shinagawa-ku, Tokyo 140, Japan, and Cancer Research Institute, Kanazawa University, Takara-machi, Kanazawa 920, Japan

Received May 3, 1995[⊗]

We have designed 2′-*C*-cyano-2′-deoxy-1-β-D-*arabino*-pentofuranosylcytosine (CNDAC) as a potential mechanism-based DNA-strand-breaking nucleoside, which showed potent tumor cell growth inhibitory activity against various human tumor cell lines in vitro and in vivo. When measuring the pK_a of the 2′α-proton of CNDAC, we found that CNDAC epimerized to 2′-*C*-cyano-2′-deoxy-1-β-D-*ribo*-pentofuranosylcytosine (CNDC) with concomitant degradation of both CNDAC and CNDC to cytosine and 1,4-anhydro-2-*C*-cyano-2-deoxy-D-*erythro*-pent-1-enitol. Kinetic analysis of these reactions showed that abstraction of the acidic 2′-proton of CNDAC and CNDC initiated the reactions, which quickly reached an equilibrium. In the equilibrium, a concentration ratio of CNDAC and CNDC was about 3:5. Concomitant degradation of these nucleosides was found to be rather slow. Deuterium incorporation experiments with CNDAC in a D_2O buffer suggested the mechanism of the β-elimination reactions is an E1cB type. These epimerization and degradation reactions were found even in neutral conditions (pH 7.5) and also occurred in RPMI 1640 cell culture medium. The discovery of which nucleoside possesses the predominate tumor cell growth inhibitory activity was important. While both nucleosides showed potent tumor cell growth inhibitory activity against three human tumor cell lines (colon carcinoma WiDr, small cell lung carcinoma SBC-5, and stomach carcinoma MKN-74 cells) in 48 h of incubation, in 20 min of incubation, CNDAC was 11–50 times more effective than CNDC. In vivo antileukemic activity of these nucleosides against a mouse P388 model, CNDAC was obviously superior to CNDC. Therefore, tumor cell growth inhibitory activity of CNDC could be related to the quantity of CNDAC produced in the tumor cells by the equilibrium initiated by the abstraction of the acidic 2′-proton of CNDC.

We have reported the design and synthesis of 2′-*C*-cyano-2′-deoxy-1-β-D-*arabino*-pentofuranosylcytosine (CNDAC) as an antitumor nucleoside antimetabolite with a potential mechanism-based DNA-strand-breaking ability.[2-4] Our hypothesis is that introduction of a cyano group as an electron-withdrawing group into the 2′β-position of 2′-deoxycytidine would greatly increase the acidity of the 2′α-proton. If CNDAC is enzymatically phosphorylated to the corresponding 5′-triphosphate and then incorporated into DNA molecules, the 2′α-proton is in the β-position to the 3′-phosphate diester and also the β-position to the 1′-position where the electron-withdrawing nucleobase is attached in the nucleotide. In this case, a β-elimination reaction would happen to produce a DNA strand break (path A) or formation of an abasic site (path B) as shown in Figure 1. CNDAC was quite cytotoxic to various human tumor cells including sarcomas, osteosarcomas, fibroblastomas, and carcinomas in vitro[2-5] with a unique spectrum different from that of a structurally related antileukemic nucleoside antimetabolite, 1-β-D-arabinofuranosylcytosine (araC).[6-8] CNDAC also had a prominent antitumor activity toward P388 mouse leukemia (*T/C* value

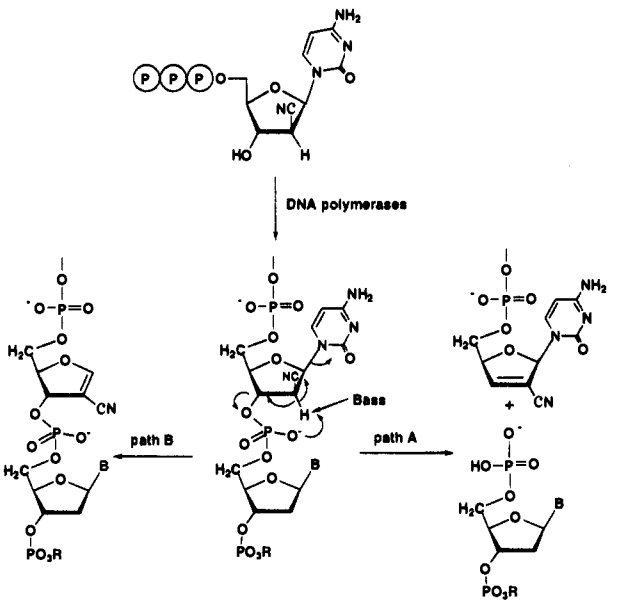

Figure 1. Possible reaction pathways of a DNA-containing CNDAC.

* Author to whom correspondence should be addressed.
† Hokkaido University.
‡ Biological Research Laboratories, Sankyo Co., Ltd.
§ Product Development Laboratories, Sankyo Co., Ltd.
∥ Kanazawa University.
⊗ Abstract published in *Advance ACS Abstracts*, August 1, 1995.

0022-2623/95/1838-3391$09.00/0

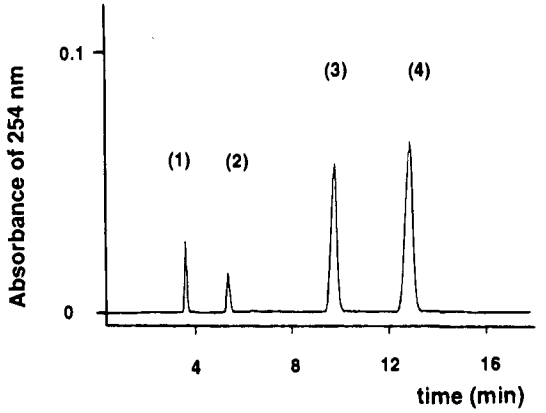

Figure 2. HPLC profiles of the reaction of CNDAC in Tris·HCl buffer (10 mM, pH 9.0, 2 h at 37 °C). For experimental conditions, see the Experimental Section. Peaks 1–4 correspond to cytosine, 1,4-anhydro-2-*C*-cyano-2-deoxy-D-*erythro*-pent-1-enitol (glycal), CNDAC, and CNDC, respectively.

> 600%)[2] and M5076 mouse reticulum cell sarcoma in vivo.[3] CNDAC also showed excellent antitumor activity against HT-1080 human fibrosarcoma, which is refractory to araC, in chick embryos or athymic mice.[5] Whether our hypothesis accurately describes the mechanism of antitumor activity is a question we would like to answer.

We found that when N^4-acetyl-CNDAC was treated with NH_3/MeOH at room temperature, the glycosyl bond was cleaved.[2,3] β-Elimination reactions produced a 2′-*C*-cyano-2′,3′-didehydro-2′,3′-dideoxycytidine derivative when a 5′-protected CNDAC was treated with *N*,*N*-thiocarbonyldiimidazole[9] in DMF at room temperature. Upon treatment with *N*,*N*-carbonyldiimidazole under the same conditions, the dehydrated product was also obtained.[2,3] These reactions proceed intramolecularly from the 3′-thiocarbonylimidazole ester or the 3′-carbonylimidazole ester. Although these reactions are model studies, it is easy to imagine that the 2′α-proton of CNDAC would have enough acidity to break DNA strands intramolecularly and/or intermolecularly when it is incorporated into DNA molecules. When we tried to measure the pK_a value of the 2′α-proton of CNDAC, we found epimerization of the 2′β-cyano group in CNDAC to give 2′-*C*-cyano-2′-deoxy-1-β-D-*ribo*-pentofuranosylcytosine (CNDC) under even very weakly alkaline conditions, followed by glycosyl bond cleavage to release the cytosine. This paper deals with detailed studies on the epimerization and degradation of CNDAC and also the inhibitory effects of the epimerized product, CNDC, compared with CNDAC, on tumor cell lines in vitro as well as in vivo.

Results and Discussion

Epimerization and Degradation of CNDAC. CNDAC was incubated in Tris·HCl buffer (10 mM, pH 9.0) at 37 °C, and the reaction mixture was analyzed by HPLC after 2 h of incubation. As shown in Figure 2, there are four peaks in the chromatograph. Structures of the compounds corresponding to each HPLC-isolated peak were assigned by their ^{1}H-NMR, IR, and MS spectra together with elemental analyses. The compounds corresponding to peak 1 and peak 3 were assigned as cytosine and CNDAC, respectively, by comparison with authentic samples. The oily material obtained from peak 2 had absorbance at 2220 cm^{-1} (CN) in its IR spectrum and a molecular ion peak at *m/z* 142 ($M^+ + 1$) in its MS spectrum. One vinylic proton signal at 7.27 ppm as a singlet due to H-1 was observed in its ^{1}H-NMR spectrum. From these data along with elemental analysis, the compound was assigned as 1,4-anhydro-2-*C*-cyano-2-deoxy-D-*erythro*-pent-1-enitol (glycal), which would be produced by a β-elimination reaction from the 2′-proton to release cytosine (Figure 4). The compound obtained from peak 4 showed a peak due to a CN group at 2250 cm^{-1} in its IR spectrum and a molecular ion peak at *m/z* 253 ($M^+ + 1$) in its MS spectrum. One doublet peak due to H-1′ was observed at 6.19 ppm with a $J_{1',2'}$ value of 7.3 Hz, and a double doublet peak due to H-2′ was detected at 3.63 ppm with $J_{2',1'}$ and $J_{2',3'}$ values of 7.3 and 6.8 Hz, respectively. In NOE experiments of the compound, irradiation of H-2′ increased H-6 (8.5%) at the cytosine base and only a 0.6% increase was observed at H-1′. In similar experiments on CNDAC, an increase at H-1′ (14.1%) but not at H-6 was observed when H-2′ was irradiated. Therefore, the cyano group is attached to the 2′α-position, and the structure of the compound obtained from peak 4 was assigned as 2′-*C*-cyano-2′-deoxy-1-β-D-*ribo*-pentofuranosylcytosine (CNDC). The product ratio of cytosine, the glycal, CNDAC, and CNDC was calculated as 1:1:3.8:5.2 from each peak area corrected by each extinction coefficient. When the isolated CNDC was also incubated under the same conditions for 2 h, cytosine, the glycal, CNDAC, and CNDC were also detected by HPLC analyses in a ratio of 1:1:3:5, respectively (data not shown).

Time profiles of the decrease of CNDAC and formation of CNDC and cytosine were examined at pH 9.0, and the results are shown in Figure 3A. Experiments using CNDC under the same conditions were also done (Figure 3B). A biphasic curve was observed in both reactions, and the other epimer was also observed in an early stage, indicating that epimerization occurs in both directions. It should be noted that the epimerization of CNDAC to CNDC in the early stage was much faster than that of CNDC to CNDAC. In the early stage, elimination of the 2′-proton and formation of the other epimer coincide. The rapid and slow stages are thus considered to reflect the epimerization and decomposition processes, respectively. If this is the case, the epimerization of CNDAC to CNDC might be faster than the opposite process. Indeed, the concentration ratio of CNDAC to CNDC is approximately 3:5 in the slow phase, confirming that CNDC is thermodynamically more stable than CNDAC. The stability of CNDAC could be feasibly explained by energy minimization in the trans configuration between the glycosyl bond and the cyano group. When the decomposition products, cytosine and glycal, were mixed under the same experimental conditions, the parent compounds, CNDAC and CNDC, were not detected with the HPLC technique, confirming that the decompositions of CNDAC and CNDC are irreversible. Therefore, both the reactions are uniformly initiated by abstraction of the acidic 2′-proton of CNDAC and CNDC (Figure 4). Assuming that the acidic 2′-proton is rapidly abstracted, an overall reaction scheme can be illustrated in the simple model in Figure 5.

To confirm the reaction scheme, the time profiles for the eliminations of the 2′-proton in CNDAC and CNDC

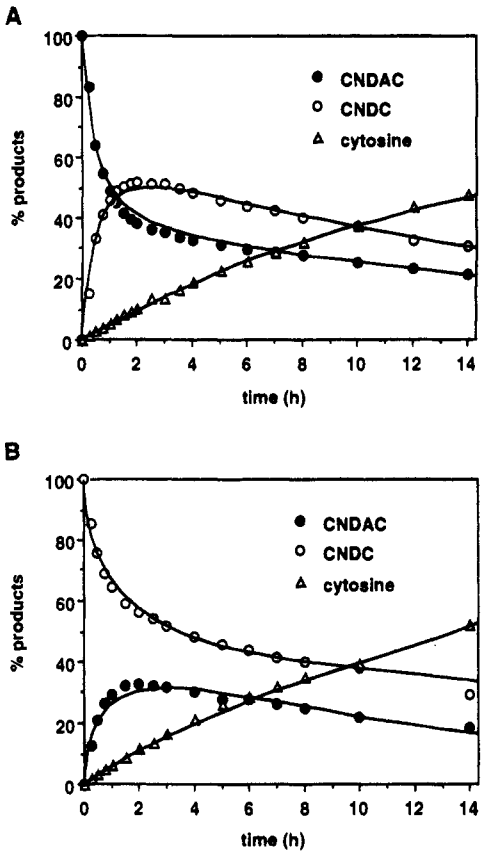

Figure 3. Time profiles and curve fitting of the epimerization and degradation reactions of CNDAC (A) and CNDC (B) in Tris·HCl buffer (10 m M, pH 9.0 at 37 °C). For experimental conditions, see the Experimental Section. Symbols indicated experimental values, and bold lines indicated theoretical values calculated from eqs 4–9 (see the Experimental Section) using the model described in Figure 5.

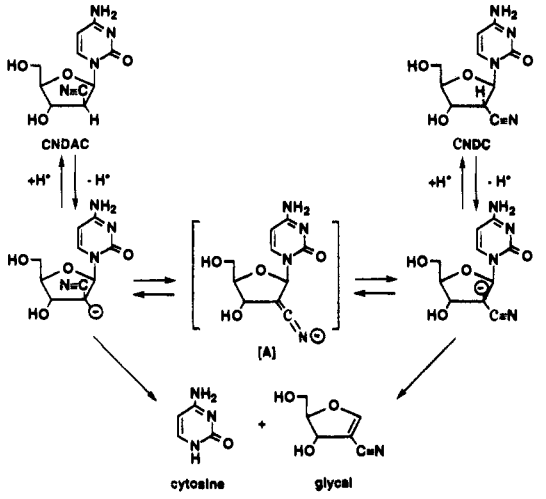

Figure 4. Possible equilibrium and degradation pathways of CNDAC and CNDC.

in 10 mM Tris·HCl buffer (pH 9.0) were kinetically analyzed based on the model shown in Figure 5, in which processes were minimized for the sake of simplicity. Kinetic parameters (k_{12}, k_{21}, k_{13}, and k_{23}) were calculated with a nonlinear least-squares method (MULTI)[11] by fitting the time profiles of concentrations of CNDAC, CNDC, and cytosine to eqs 4–9 (see the Experimental Section). The fitted curves are shown in Figure 3. The Akaike's information criterion (AIC)[12,13] values were −108 and −166 when the starting materials

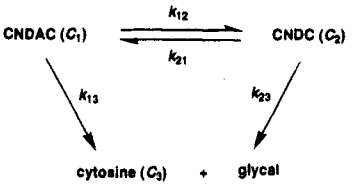

Figure 5. Model for the equilibrium and degradation reactions.

were CNDAC and CNDC, respectively. The calculated and experimental data are well correlated. The k_{12} and k_{21} values were 0.88 and 0.60 h^{-1}, respectively, when CNDAC was used as a starting material. As aforementioned, the equilibrium between CNDAC and CNDC inclined toward CNDC. When CNDC was used as a starting material, the k_{12} and k_{21} values were 1.08 and 0.64 h^{-1}, respectively. However, the calculated values for decompositions (k_{13} and k_{23}) depended on the starting materials. For example, the k_{13} and k_{23} values were 0.058 and 0.043 h^{-1} (CNDAC as a starting material) and 0.011 and 0.078 h^{-1} (CNDC as a starting material). When CNDC was used as a starting material, the decomposition of the other epimer, CNDAC, was rather underestimated. What mechanisms account for this discrepancy? A feasible mechanism is that the glycosyl bond cleavage to produce cytosine would also proceed through an intermediate [A] (Figure 4), which is formed by the deprotonation of the 2'-proton (Figure 4). To discover whether intermediate [A] exists, CNDAC was incubated in a D_2O buffer (pD 8.0). More than 99% of both CNDAC and CNDC isolated from the reaction mixture by HPLC contained a deuterium atom at the corresponding 2'-position. A part of the ^{1}H-NMR spectra of these deuterated nucleosides is shown in Figure 6. For an explanation for the deuterium replacement it is necessary to consider the E1cB type elimination mechanism,[10] in which there is an intermediate [A]. Strictly speaking, the time profiles of CNDAC and CNDC degradations thus have to be analyzed based on the model, in which the intermediate is additionally incorporated. However, the more kinetic parameters which are considered, the more difficult the analysis. The algebraic sum of k_{13} and k_{23} values remained unchanged irrespective of the starting material. For convenience sake, this sum was adopted as the total decomposition rate constant.

Epimerization and glycosyl bond cleavage processes are started by the abstraction of the acidic 2'-proton of CNDAC and CNDC. All kinetic parameters were thus considered to be dependent on the buffer pH. We then demonstrated the effects of buffer pH on the kinetic parameters, which are summarized in Table 1. All kinetic parameters were increased as the pH increased, indicating that the parameters reflect the 2'-deprotonation. To calculate the pK_a of the 2'-proton, the k_{12} values were plotted vs pH, as shown in Figure 7. Unfortunately, no plateau was observed in the pH relationship, since over pH 12, the reactions were too fast to accurately detect each product by HPLC. It is worth noting that abstraction of the 2'-proton reached an equilibrium between the epimers even in the pH 7.5 buffer after 25 h at 37 °C. As shown in Table 2, all the processes were also accelerated when salt concentrations were changed to 0.01–1 M in the buffer (pH 9.0) used. Taken together, the 2'-proton of CNDAC or CNDC has a rather higher acidity than that of normal

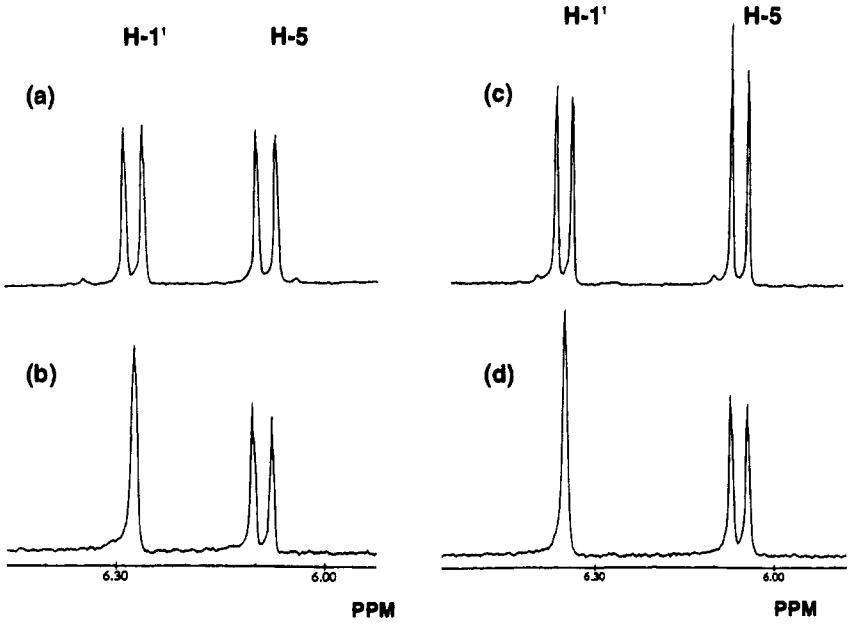

Figure 6. Parts of ^{1}H-NMR spectra of CNDAC (a), 2′-D-CNDAC (b), CNDC (c), and 2′-D-CNDC (d) in D_2O.

Table 1. Kinetic Parameters of the Epimerization and the Degradation Reactions of CNDAC at Various pH in Tris·HCl Buffer (10 mM) at 37 °C[a]

pH	k_{12} (h^{-1})	k_{21} (h^{-1})	$k_{13}+k_{23}$ (h^{-1})	$t_{1/2}$ (h) of CNDAC
7.5	0.062	0.037	0.009	38
8.0	0.22	0.14	0.02	4
9.0	0.88	0.60	0.09	1
9.6	2.14	1.41	0.26	0.45
10.0	6.18	4.07	0.69	0.14
10.6	28.4	16.3	4.05	0.033
11.3	101.5	68.5	11.6	0.009

[a] For the reaction conditions and calculation of the kinetic parameters, see the Experimental Section.

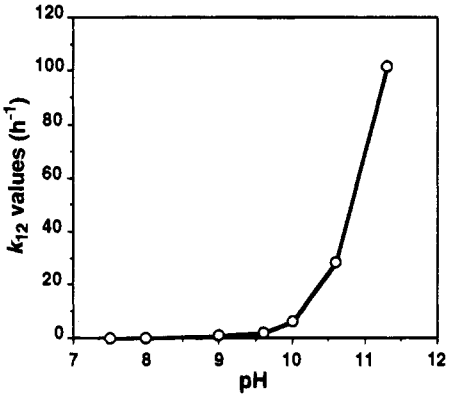

Figure 7. Relationship between the k_{12} and pH for the epimerization of CNDAC.

Table 2. Kinetic Parameters of the Epimerization and the Degradation Reactions of CNDAC at Various Salt Concentrations in Tris·HCl Buffer (pH 9.0) at 37 °C[a]

conc (M)	k_{12} (h^{-1})	k_{21} (h^{-1})	$k_{13}+k_{23}$ (h^{-1})	$t_{1/2}$ (h) of CNDAC
0.01	0.88	0.60	0.09	1
0.1	1.88	1.16	0.19	0.5
1.0	2.31	1.35	0.30	0.35

[a] For the reaction conditions and calculation of the kinetic parameters, see the Experimental Section.

nucleosides, and the abstraction can occur in blood and the tumor cells. This property would be reflected in its antitumor activity.

Antitumor Activity of CNDAC and CNDC. We had reported tumor cell growth inhibition of CNDAC against various human tumor cell lines in vitro after 72 h of incubation.[3,5] However, as described above, CNDAC is epimerized to CNDC even under neutral conditions, and such epimerization also occurred quickly under high salt concentrations. It is important to find whether CNDAC or CNDC is responsible for the tumor cell growth inhibitory activity. Therefore, CNDAC was incubated in RPMI 1640 cell culture medium (pH of the medium about 7.5) containing 10% fetal calf serum at 37 °C. As shown in Figure 8, CNDAC was obviously epimerized to CNDC, reaching equilibrium at 8 h of incubation, with concomitant decomposition of CNDAC and CNDC to cytosine and the glycal. Although this experiment may not accurately reflect events in tumor cells, such epimerization and decomposition reactions would happen to some extent in tumor cells.

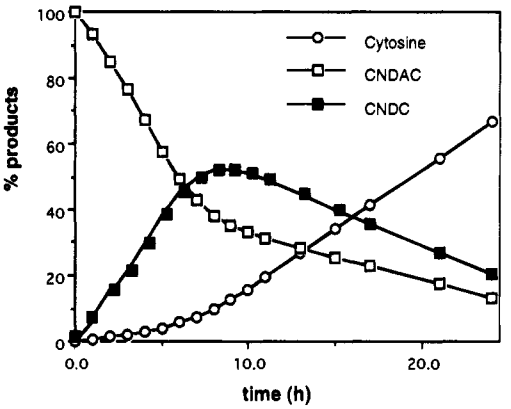

Figure 8. Time profiles of the epimerization and degradation reactions of CNDAC in RPMI 1640 cell culture medium.

We reinvestigated the tumor cell growth inhibitory activity of CNDAC and CNDC against three human solid tumor cell lines (colon carcinoma WiDr, small cell lung carcinoma SBC-5, and stomach carcinoma MKN-74 cell lines) treated for 20 min or 48 h, and then the cells were washed with medium and incubated for 6 days from the addition of drugs. The results are shown in Table 3. While, for 48 h of drug exposure, both

Table 3. In Vitro Cell Growth Inhibitory Activity of CNDAC and CNDC against Human Colon Carcinoma WiDr, Small Cell Lung Carcinoma SBC-5, and Stomach Carcinoma MKN-74 Cell Lines under 20 min and 48 h Exposures

	IC_{50} (μM)[b]			
	20-min exposure		48-h exposure	
cell line	CNDAC	CNDC	CNDAC	CNDC
WiDr[a]	16.5	436	0.157	0.306
SBC-5[a]	7.14	360	0.222	0.367
MKN-74[a]	24.9	265	0.150	0.206

[a] WiDr (5×10^2 cells), SBC-5 (2.5×10^2 cells), and MKN-74 (1×10^3 cells) were used. [b] IC_{50} values were given as the concentration required for 50% inhibition of cell growth.

CNDAC and CNDC showed almost equal potency toward all three cell lines, CNDC was 11–50 times less effective than CNDAC for 20 min of drug exposure. In the 20-min exposure experiments, as shown in Figure 8, both CNDAC and CNDC are calculated to be epimerized less than 5% to each other, but, after 48 h of incubation, both had reached equilibrium. Since, in separate experiments, both cytosine and the glycal did not show any tumor cell growth inhibitory activity up to 100 μg/mL against cell lines used in this study, tumor cell growth inhibitory activity of CNDC mainly would be related to the epimerized CNDAC. The IC_{50} values for CNDAC itself would be much lower than the apparent ones, since CNDAC is also epimerized and decomposed in the medium as well as in the cells. Usually, 2'-deoxycytidine derivatives having a substituent at the 2'α-position are less effective than the corresponding nucleosides having a substituent at the 2'β-position.[4] This would be related to substrate specificity of certain kinases, such as uridine–cytidine kinase and deoxycytidine kinase.

We also evaluated the in vivo antileukemic activity of CNDC against P388 mouse leukemia cells implanted intraperitoneally into female CDF_1 mice and compared the activity with that of CNDAC (Table 4). When CNDC was administered intraperitoneally on days 1–5 at a dose of 25 mg/kg/day, it showed antileukemic activity with a *T/C* value of 138%. Increasing the dose to 200 mg/kg/day without changing the schedule gave a *T/C* value of 203%. However, even at a dose of 25 mg/kg/day under the same schedule of drug administration, CNDAC showed a *T/C* of 300%, and at a dose of 200 mg/kg/day, the *T/C* value was increased to 333%. Therefore, CNDAC was much more potent than CNDC, and the activity of CNDC would be related to the quantity of CNDAC produced in the tumor cells by the equilibrium started by the abstraction of the acidic 2'-proton of CNDC.

In conclusion, the chemical stability of CNDAC was investigated in an alkaline buffer and we found that there was an equilibrium between CNDAC and CNDC, rather than concomitant degradation of these epimers to cytosine, and the glycal was also observed. CNDC showed similar phenomena. These reactions were initiated by the abstraction of the acidic 2'-proton, and the mechanism of the β-elimination reaction was confirmed as an ElcB mechanism by deuterium incorporation experiments. While CNDC and CNDAC showed similar potent tumor cell growth inhibitory activity against human solid tumor cell lines in vitro when incubated for 48 h, in short-exposure experiments, CNDC was 11–50 times less potent than CNDAC. Therefore, CNDC was converted to CNDAC, which had tumor cell growth inhibitory activity. The in vivo antileukemic activity of CNDC was also compared with that of CNDAC, and we found CNDAC has much stronger antileukemic potency, which would also be suggested by the epimerization and degradation in vitro experiments.

Table 4. In Vivo Antileukemic Activity of CNDC and CNDAC against P388 Mouse Leukemic Cells by ip Administration in Mice[a]

	dose (mg/kg/day)	weight change (g)[b]	*T/C*[c] (%)
CNDC	200	+0.9	203
	100	+0.7	180
	50	+0.9	164
	25	+1.6	138
CNDAC	200	−2.5	333
	100	−2.8	311
	50	−2.1	300
	25	+0.3	300
control		+3.3	100

[a] P388 cells (10^6) were implanted ip to female CDF_1 mice (n = 6), and each drug was given ip on days 1–5. [b] The changes in body weight of mice were obtained by subtracting the average weight on day 1 from that on day 7. [c] The ratio of treated mice (*T*) vs control mice (*C*) in median survival time was calculated. Median survival of untreated control mice was 9.0 days.

Experimental Section

Melting points were measured on a Yanagimoto MP-3 micromelting point apparatus and are uncorrected. Fast atom bombardment mass spectrometry (FAB-MS) was done on a Jeol JMS-HX110 at an ionizing voltage of 70 eV. The ^1H NMR spectra were recorded on a Jeol JNM-GX 270 (270 MHz) spectrometer or Bruker ARX 500 (500 MHz) spectrometer with 3-(trimethylsilyl)propanesulfonic acid sodium salt as an internal standard. Chemical shifts are reported in parts per million (δ), and signals are expressed as s (singlet), d (doublet), t (triplet), m (multiplet), or br (broad). UV absorption spectra were recorded with a Shimadzu UV-240 spectrophotometer. IR spectra were recorded with a Jeol A-102 spectrometer. HPLC was done using a Shimadzu LC-6A unit.

Isolation of CNDAC, CNDC, and the Glycal. A solution of CNDAC·HCl (30 mg, 0.10 mmol) in 0.1 M Tris·HCl buffer (pH 10, 1 mL) was incubated for 6 h at 37 °C. The mixture was analyzed by the analytical ODS column described as above. These compounds were separated by a preparative ODS column (YMC D-ODS-5, 20 × 250 mm) to give 1,4-anhydro-2-*C*-cyano-2-deoxy-D-*erythro*-pent-1-enitol (glycal; 4.5 mg, 28% as a syrup) and 2'-*C*-cyano-2'-deoxy-1-β-D-*ribo*-pentofuranosylcytosine (CNDC; 10.5 mg, 33% as a powder, which was converted to an HCl salt by coevaporation several times with 1 M HCl in EtOH. The glycal (15 mg, 92% as a syrup) was obtained when the above mixture was incubated for 18 h. Physical data for the glycal: FAB-MS *m/z* 142 ($M^+ + 1$, 6%); IR (D_2O) 2220 cm^{-1}; ^1H-NMR (D_2O) 7.27 (1 H, s, H-1), 5.05 (1 H, d, H-3, $J_{3,4}$ = 3.7 Hz), 4.65 (1 H, ddd, H-4, $J_{4,3}$ = 3.7, $J_{4,5a}$ = 4.0, $J_{4,5b}$ = 5.1 Hz), 3.85 (1 H, dd, H-5a, $J_{5a,4}$ = 4.0, $J_{a,b}$ = 12.1 Hz), 3.77 (1 H, dd, H-5b, $J_{5b,4}$ = 5.1, $J_{b,a}$ = 12.1 Hz). Anal. ($C_6H_7NO_3 \cdot {}^1/_{18}H_2O$) C, H, N. Physical data for CNDC·HCl: mp 193–194 °C; IR (MeOH) 2250 cm^{-1}; ^1H-NMR (D_2O) 7.62 (1 H, d, H-6, $J_{6,5}$ = 7.8 Hz), 6.19 (1 H, d, H-1', $J_{1',2'}$ = 7.3 Hz), 5.90 (1 H, H-5, $J_{5,6}$ = 7.8 Hz), 4.43 (1 H, dd, H-3', $J_{3',2'}$ = 6.8, $J_{3',4'}$ = 6.4 Hz), 4.05 (1 H, dd, H-4', $J_{4',3'}$ = 6.4, $J_{4',5'a}$ = 3.4, $J_{4',5'b}$ = 2.9 Hz), 3.70 (1 H, dd, H-5'a, $J_{5'a,4'}$ = 3.4, $J_{a,b}$ = 12.7 Hz), 3.63 (1 H, dd, H-2', $J_{2',1'}$ = 7.3, $J_{2',3'}$ = 6.8 Hz), 3.61 (1 H, dd, H-5'b, $J_{5'b,4'}$ = 2.9, $J_{b,a}$ = 12.7 Hz). Anal. ($C_{10}H_{13}N_4O_4HCl \cdot {}^1/_4MeOH$) C, H, N. Physical data for CNDAC·HCl: mp 175–176 °C; IR (MeOH) 2270 cm^{-1}; ^1H-NMR (D_2O) 7.71 (1 H, d, H-6, $J_{6,5}$ = 7.8 Hz), 6.12 (1 H, d, H-1', $J_{1',2'}$ = 7.3 Hz), 5.93 (1 H, d, H-5, $J_{5,6}$ = 7.8 Hz), 4.49 (1 H, dd, H-3', $J_{3',2'}$ = 6.8, $J_{3',4'}$ = 7.3 Hz), 3.88 (1 H, ddd, H-4', $J_{4',3'}$ = 7.3, $J_{4',5'a}$ = 2.9, $J_{4',5'b}$ = 4.9 Hz), 3.82 (1 H, dd, H-5'a, $J_{5'a,4'}$ = 2.9,

$J_{a,b}$ = 13.2 Hz), 3.77 (1 H, dd, H-2', $J_{2',1'}$ = 7.3, $J_{2',3'}$ = 6.8 Hz), 3.68 (1 H, dd, H-5'b, $J_{5'b,4'}$ = 4.9, $J_{b,a}$ = 13.2 Hz). Anal. ($C_{10}H_{13}N_4O_4$·HCl·$^1/_2$EtOH) C, H, N.

Isolation of 2'-D-CNDAC and 2'-D-CNDC. A solution of CNDAC (6 mg, 0.024 mmol) in 0.1 M Tris·HCl buffer in D_2O (pD 8, 1 mL) was incubated for 8 h at 37 °C. [2'α-^{2}H]-2'-*C*-Cyano-2'-deoxy-1-β-D-*arabino*-pentofuranosylcytosine (2'-D-CNDAC; 1.8 mg, 30% as white foam) and [2'β-^{2}H]-2'-*C*-cyano-2'-deoxy-1-β-D-*ribo*-pentofuranosylcytosine (2'-D-CNDC; 2.5 mg, 42% as white foam) were separated by HPLC with a C-18 silica gel column (YMC-D-ODS-5, 20 × 250 mm) with aqueous 5% MeOH at a flow rate of 1 mL/min. Peaks corresponding to 2'-CNDAC and 2'-D-CNDC was detected at 254 nm and showed retention times of 8.0 and 11.1 min, respectively. Physical data for 2'-D-CNDAC: FAB-MS *m/z* 258 (M^+ + 1, 10%); ^{1}H-NMR (D_2O) 7.88 (1 H, d, H-6, $J_{6,5}$ = 7.5 Hz), 6.27 (1 H, s, H-1'), 6.08 (1 H, d, H-5, $J_{5,6}$ = 7.5 Hz), 4.65 (1 H, d, H-3', $J_{3',4'}$ = 7.3 Hz), 4.04 (1 H, dt, H-4', $J_{4',3'}$ = 7.3, $J_{4',5'a}$ = 2.8, $J_{4',5'b}$ = 4.7 Hz), 3.95 (1 H, dd, H-5'a, $J_{5'a,4'}$ = 2.8, $J_{a,b}$ = 12.8 Hz), 3.83 (1 H, dd, H-5'b, $J_{5'b,4'}$ = 4.7, $J_{b,a}$ = 12.8 Hz). Physical data for 2'-D-CNDC: FAB-MS *m/z* 258 (M^+ + 1, 10%); ^{1}H-NMR (D_2O) 7.76 (1 H, d, H-6, $J_{6,5}$ = 7.5 Hz), 6.33 (1 H, s, H-1'), 6.03 (1 H, d, H-5, $J_{5,6}$ = 7.5 Hz), 4.58 (1 H, d, H-3', $J_{3',4'}$ = 3.8 Hz), 4.20 (1 H, dt, H-4', $J_{4',3'}$ = 3.8, $J_{4',5'a}$ = 3.0, $J_{4',5'b}$ = 4.3 Hz), 3.85 (1 H, dd, H-5'a, $J_{5'a,4'}$ = 3.0, $J_{a,b}$ = 12.7 Hz), 3.83 (1 H, dd, H-5'b, $J_{5'b,4'}$ = 4.3, $J_{b,a}$ = 12.7 Hz).

Kinetic Analysis. A solution of CNDAC or CNDC (3 mg, 0.012 mmol) in Tris·HCl buffer (pH 7.5–10.3, 0.01–1 M, 1 mL) or in RPMI 1640 cell culture medium containing 10% FCS (1 mL) was incubated at 37 °C. At appropriate periods, samples of the reaction mixture (5 mL) were analyzed by HPLC with the C-18 silica gel column (Inertsil ODS-2, GL Science Inc., 4.6 × 250 mm) with 2.5% aqueous MeOH as an eluting solvent at a flow rate of 1 mL/min. Each peak corresponding to cytosine, the glycal, CNDAC, and CNDC was detected at 254 nm and showed retention times of 3.8, 5.3, 9.8, and 12.8 min, respectively. Each peak area ratio was calculated using the values of ϵ = 7000 for CNDAC and CNDC and ϵ 4600 for cytosine at 254 nm. The time profiles for the equilibrium and the decomposition of CNDAC and CNDC were kinetically analyzed on the model shown in Figure 5. Kinetic parameters (k_{12}, k_{21}, k_{13}, and k_{23}) were calculated with a nonlinear least-squares method by fitting the time profiles for the concentration of CNDAC (C_1), CNDC (C_2), and cytosine (C_3) with eqs 1–3, which were further converted to eqs 4–9 using a computer software MULTI.[11]

Compartment Analysis. Time profiles of the degradation of CNDAC and CNDC were analyzed based on the simple model (Figure 5). The principle of mass–balance results in the following differential equations:

$$V(dC_1/dt) = -\{(k_{12} + k_{13})C_1 + K_{21}C_2\}V \quad (1)$$

$$V(dC_2/dt) = -\{(k_{21} + k_{23})C_2 + k_{12}C_1\}V \quad (2)$$

$$V(dC_3/dt) = \{k_{13}C_1 + k_{23}C_2\}V \quad (3)$$

where C_1 represents the CNDAC concentration, C_2 the CNDC concentration, C_3 the cytosine concentration, k_{12} the rate constant of epimerization from CNDAC to CNDC, k_{21} the rate constant of epimerization from CNDC to CNDAC, k_{13} the rate constant of CNDAC decomposition, k_{23} the rate constant of CNDC decomposition, and V the reservoir volume.

Using the Laplace transformation, these differential eqs 1–3 were analytically solved to become the following equations (eqs 4–9). Kinetic parameters in the model were calculated with a nonlinear least-squares method (MULTI)[11] by fitting the time profiles for CNDAC, CNDC, and cytosine to eqs 4–9. Starting from CNDAC:

$$C_1 = 100[(k_{21} + k_{23} - \alpha)/(\beta - \alpha)\exp(-\alpha t) + (k_{21} + k_{23} - \beta)/(\alpha - \beta)\exp(-\beta t)] \quad (4)$$

$$C_2 = 100[k_{12}/(\beta - \alpha)\exp(-\alpha t) + k_{12}/(\alpha - \beta)\exp(-\beta t)] \quad (5)$$

$$C_3 = 100[1 + (\beta - k_{13})/(\alpha - \beta)\exp(-\alpha t) + (\alpha - k_{13})/(\beta - \alpha)\exp(-\alpha t)] \quad (6)$$

Starting from CNDC:

$$C_1 = 100[k_{21}/(\beta - \alpha)\exp(-\alpha t) + k_{21}/(\alpha - \beta)\exp(-\beta t)] \quad (7)$$

$$C_2 = 100[(k_{12} + k_{13} - \alpha)/(\beta - \alpha)\exp(-\alpha t) + (k_{12} + k_{13} - \beta)/(\alpha - \beta)\exp(-\beta t)] \quad (8)$$

$$C_3 = 100[1 + (\beta - k_{23})/(\alpha - \beta)\exp(-\alpha t) + (\beta - \alpha)\exp(-\alpha t)] \quad (9)$$

$$\alpha = 0.5\{(k_{12} + k_{13} + k_{23} + k_{21}) + [(k_{12} + k_{13} + k_{23} + k_{21})^2 - 4(k_{12}k_{23} + k_{13}k_{23} + k_{13}k_{21})]^{0.5}\}$$

$$\beta = 0.5\{(k_{12} + k_{13} + k_{23} + k_{21}) - [(k_{12} + k_{13} + k_{23} + k_{21})^2 - 4(k_{12}k_{23} + k_{13}k_{23} + k_{13}k_{21})]^{0.5}\}$$

Goodness of the fitting was estimated by Akaike's information constant (AIC) values.[12,13]

Cell Growth Inhibitory Activity of CNDC and CNDAC in Vitro. The human colon adenocarcinoma WiDr was obtained from American Type Culture Collection. The human small cell lung carcinoma SBC-5 was obtained from the Japanese Cancer Research Resources Cell Bank (Tokyo, Japan). Human gastric adenocarcinoma MNK-74 was obtained from Immuno-Biological Laboratories (Gunma, Japan). The tetrazolium-based semiautomated colorimetric assay (MTT assay)[14] was used for the in vitro assay. 5 × 10^2 WiDr cells, 2.5 × 10^2 SBC-5 cells, or 1 × 10^3 MKN-74 cells in 100 mL of medium were seeded into 96-well flat-bottom microwell plates (InterMed, Roskilde, Denmark) and incubated for 24 h at 37 °C in a humidified atmosphere of 5% CO_2. Then 100 μL of CNDAC·HCl and CNDC·HCl solutions with graded concentrations was added in tetraplicate to each well, and the plates were incubated for 20 min or 48 h in a humidified atmosphere of 5% CO_2. Then the plates were washed with 200 μL of medium three times and were incubated for 6 days from addition of drugs. Five milligrams of MTT [3-(4,5-dimethylthiazol-2-yl)-2,5-diphenyltetrazolium bromide; Dohindo, Kumamoto, Japan] was dissolved in 1 mL of PBS, was filtered with 0.45-μm filter units (Millipore; Bedford, MA), and was diluted with 4 mL of the medium. Fifty microliters of MTT solution (1 mg/mL) was added to each well. After incubation for 4 h at 37 °C, the medium was removed by aspiration, 150 μL of DMSO was added to each well, and the plates were shaken with a mechanical plate shaker for 5 min. Absorbance at 540 nm was measured with a ImmunoReader NJ-2000 (InterMed Japan; Tokyo, Japan). The percentage of cell growth inhibition was calculated by the following formula: % of cell growth inhibition = (1 − *T*/*C*) × 100, where *C* is the mean OD_{540} of the control group and *T* is that of the treated group. The 50% inhibitory drug concentration (IC_{50} value) was calculated graphically from the dose–response curve.

Antileukemic Activity of CNDC and CNDAC in Vivo. Mouse leukemia P388 cells were obtained from Japanese Foundation for Cancer Research (Tokyo, Japan) and were maintained by passaging intraperitoneally (ip) weekly to female DBA/2 mouse (Charles River Japan, Inc.; Kanagawa, Japan) in a specific pathogen-free area. Just before administration CNDC·HCl or CNDAC·HCl was dissolved and diluted in saline to give 0.1 mL/10 g of body weight of mice. Viable P388 cells (1 × 10^6) were implanted ip in 6-week-old female CDF_1 mice (n = 6) (Charles River, Japan), and each drug was

given ip on days 1–5. The ratio of treated mice (*T*) vs untreated control mice (*C*) in median survival time was calculated. Body weight changes of mice were obtained by subtracting the average weight on day 1 from that on day 7.

Acknowledgment. This investigation was supported in part by Grants-in-Aid for Cancer Research and for Scientific Research on Priority Areas from the Ministry of Education, Science, and Culture of Japan.

References

(1) Part 140: Minakawa, N.; Kojima, N.; Sasaki, T.; Matsuda, A. Synthesis and antileukemic activity of 5-carbon-substituted 1-β-D-ribofuranosylimidazole-4-carboxamides. *Nucleosides Nucleotides*, in press.

(2) Matsuda, A.; Nakajima, Y.; Azuma, A.; Tanaka, M.; Sasaki, T. 2′-*C*-Cyano-2′-deoxy-1-β-D-arabinofuranosylcytosine (CNDAC): Design of a potential mechanism-based DNA-strand-breaking antineoplastic nucleoside. *J. Med. Chem.* **1991**, *34*, 2917–2919.

(3) Azuma, A.; Nakajima, Y.; Nishizono, N.; Minakawa, N.; Suzuki, M.; Hanaoka, K.; Kobayashi, T.; Tanaka, M.; Sasaki, T.; Matsuda, A. 2′-*C*-Cyano-2′-deoxy-1-β-D-arabinofuranosylcytosine (CNDAC) and its derivatives: A new class of nucleosides with a broad antitumor spectrum. *J. Med. Chem.* **1993**, *36*, 4183–4189.

(4) Matsuda, A.; Azuma, A.; Nakajima, Y.; Takenuki, K.; Dan, A.; Iino, T.; Yoshimura, Y.; Minakawa, N.; Tanaka, M.; Sasaki, T. Design of new types of antitumor nucleosides: The synthesis and antitumor activity of 2′-deoxy-(2′-*C*-substituted)cytidines. In *Nucleosides and Nucleotides as Antitumor and Antiviral Agents*; Chu, C. K., Baker, D. C., Eds.; Plenum Publishing Co.: New York, 1993; pp 1–22.

(5) Tanaka, M.; Matsuda, A.; Terao, T.; Sasaki, T. Antitumor activity of a novel nucleoside, 2′-*C*-cyano-2′-deoxy-1-β-D-arabinofuranosylcytosine (CNDAC) against murine and human tumors. *Cancer Lett.* **1992**, *64*, 67–74.

(6) Keating, M. J.; McCredie, K. B.; Bodey, G. P.; Smith, T. L.; Gehan, E.; Freidreich, E. J. Improved prospects for long-term survival in adults with acute myelogenous leukemia. *JAMA* **1982**, *248*, 2481–2486.

(7) Livingston, R. B.; Carter, S. K. Cytosine arabinoside (NSC-63878)-Clinical brochure. *Cancer Chemother. Rep.* **1968**, *1* (No. 1), Part 3 179–205.

(8) Ellison, R. R.; Holland, J. F.; Weil, M.; Jacquillant, C.; Bernard, J.; Sawitsky, A.; Rosner, F.; Gussoff, B.; Silver, R. T.; Karanas, A.; Cuttner, J.; Spurr, C. L.; Hayes, D. M.; Blom, J.; Leone, L. A.; Haurani, F.; Kyle, R.; Huchison, J. L.; Forcier, R. J.; Moon, J. H. Arabinosyl cytosine: a useful agent in the treatment of acute leukemia in adults. *Blood* **1968**, *32*, 507–523.

(9) Matsuda, A.; Satoh, M.; Nakashima, H.; Yamamoto, N.; Ueda, T. Synthesis aand anti-HIV activity of 3′-cyano-2′,3′-dideoxythymidine and 3′-cyano-2′,3′-didehydro-2′,3′-dideoxythymidine. *Heterocycles* **1988**, *27*, 2545–2548.

(10) Bordwell, F. G.; Arnold, R.; Biranowski, J. B. Steric hindrance and steric assistance to carbanion formation in ElcB elimination reactions. *J. Org. Chem.* **1963**, *28*, 2496–2498.

(11) Yamaoka, K.; Tanigawara, Y.; Nakagawa, T.; Uno, T. A pharmacokinetic analysis program MULTI for microcomputer. *J. Pharm. Dyn.* **1981**, *4*, 879–885.

(12) Akaike, H. A new look at the statistical model identification. *IEEE Trans. Aut. Contr.* **1973**, *19*, 716–723.

(13) Yamaoka, K.; Nakagawa, T.; Uno, T. Application of Akaike's information criterion (AIC) in the evaluation of linear pharmacokinetic equations. *J. Pharmacol. Biopharm.* **1978**, *6*, 165–175.

(14) Alley, M. C.; Scudiero, D. A.; Monks, A.; Hursey, M. L.; Czerwinski, M. J.; Fine, D. L.; Abbott, B. J.; Mayo, J. G.; Shoemaker, R. H.; Boyd, M. R. Feasibility of drug screening with panels of human tumor cell lines using a microculture tetrazolium assay. *Cancer Res.* **1988**, *48*, 589–601.

JM950326W